Production of $N^*(1535)$ and $N^*(1650)$ in $\Lambda_c \to \bar{K}^0 \eta p$ (πN) decay

R. Pavao,* S. Sakai, and E. Oset

Departamento de Física Teórica and IFIC, Centro Mixto Universidad de Valencia-CSIC Institutos de Investigación de Paterna, Aptdo.22085, 46071 Valencia, Spain

(Received 5 March 2018; revised manuscript received 2 May 2018; published 2 July 2018)

To study the properties of the $N^*(1535)$ and $N^*(1650)$, we calculate the mass distributions of MB in the $\Lambda_c \to \bar{K}^0 MB$ decay, with $MB = \pi N (I = 1/2)$, ηp, and $K\Sigma (I = 1/2)$. We do this by calculating the tree-level and loop contributions, mixing pseudoscalar-baryon and vector-baryon channels using the local hidden gauge formalism. The loop contributions for each channel are calculated using the chiral unitary approach. We observe that for the ηN mass distribution only the $N^*(1535)$ is seen, with the $N^*(1650)$ contributing to the width of the curve, but for the πN mass distribution both resonances are clearly visible. In the case of $MB = K\Sigma$, we found that the strength of the $K\Sigma$ mass distribution is smaller than that of the mass distributions of the πN and ηp in the $\Lambda_c^+ \to \bar{K}^0 \pi N$ and $\Lambda_c^+ \to \bar{K}^0 \eta p$ processes, in spite of this channel having a large coupling to the $N^*(1650)$. This is because the $K\Sigma$ pair production is suppressed in the primary production from the Λ_c decay.

DOI: 10.1103/PhysRevC.98.015201

I. INTRODUCTION

The nature of the $N^*(1535)$ ($J^P = 1/2^-$) remains to be well understood [1,2]. Its properties have been studied within the context of the constituent quark model [3,4], where the mass of the lowest excitation of the nucleon with a negative parity is found smaller than its positive-parity counterpart, contrary to what is observed in experiment, namely, the $N^*(1535)$ and $N^*(1440)$ resonances. This is known as the mass reverse problem. Also it seems to be difficult to explain the fact that the $N^*(1535)$ could couple to channels with strangeness, such as ηN and $K\Lambda$ [4,5], within the formalism of the quark model with a simple qqq configuration where the $\bar{s}s$ component is not contained in the $N^*(1535)$ resonance. Studies, such as the ones found in Refs. [6–10], attempt to solve some difficulties in the description of the $N^*(1535)$ properties with some extension of the conventional quark model, and the possible role of the $N^*(1535)$ resonance in some reactions is explored in Refs. [11–18].

However, by using the chiral Lagrangians within the framework of the unitary coupled channels approach, some previously unexplained baryonic resonances could be understood as meson-baryon molecular states. A well-known example of this are the studies of the $\Lambda(1405)$ that were carried out in Refs. [19–28]. In the same way, the $N^*(1535)$ resonance is studied including the ηN, πN, $K\Lambda$, and $K\Sigma$ channels. The mass and width of the $N^*(1535)$ could be obtained by calculating the position of the poles of the T matrix on the second (unphysical) Riemann sheet [29–34] and were found to be in good agreement with experiment. Using this formalism, the $N^*(1535)$ was also found to couple strongly to ηN, $K\Sigma$, and $K\Lambda$, as well as less strongly to πN. In Refs. [19,30,35], in particular, where the $N^*(1535)$ was dynamically generated through pseudoscalar meson–baryon (PB) interactions. The loop functions were renormalized using the cutoff (in Refs. [19,35]) and dimensional (in Ref. [30]) regularization schemes, and the cutoffs and subtraction constants were required to have different values for each of the coupled channels to get a good agreement with experiment. This is quite different from the case of the $\Lambda(1405)$, where only a single global cutoff was needed [21]. In the case of the dimensional regularization [30], the values of the subtraction constants are different from the "natural" size, which is related to the mass of the first resonance (the ρ meson in this case) [23]. However, from the consideration of the Castillejo-Dalitz-Dyson pole contribution, the study of Ref. [36] suggests that some contribution other than the meson–baryon component would also be important for the $N^*(1535)$.

In the vector meson-baryon system, the $N^*(1650)$ was first obtained as a degenerate state of $J^P = 1/2^-$ and $3/2^-$ in the study of the vector octet-baryon octet system with the chiral unitary approach [37]. The $J^P = 3/2^-$ case was studied in Ref. [38] with the ρN(s wave), $\pi\Delta$(s wave), πN(d wave), and $\pi\Delta$(d wave) channels, and there a pole was found that can be associated with the $N^*(1700)$ resonance, having a sizable coupling to ρN. The mixing effects of PB channels with vector meson–baryon (VB) channels with $J^P = 1/2^-$ were explored in Refs. [33,39–41] and they were found to be quite significant. In Ref. [34] the possibility that the missing component in Refs. [30,35] corresponds to VB channels was explored by introducing the ρN(s wave) and $\pi\Delta$(d wave) states in the model of Ref. [30] using the local hidden gauge formalism. Doing this, both the $N^*(1535)$ and $N^*(1650)$ ($J^P = 1/2^-$) resonances were dynamically generated, and the masses and widths obtained were very close to their experimental values. Also the subtraction constants used in that study, although still different for each channel, were now very close to a "natural" value. A similar work to this was done in Ref. [33]. The two resonances were also generated in Refs. [29,31] using only

*rpavao@ific.uv.es

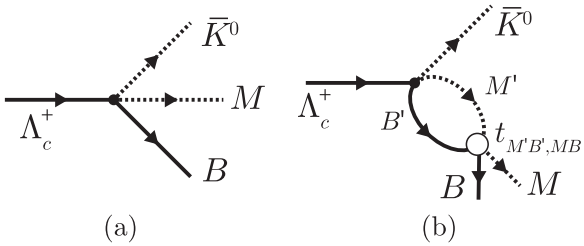

FIG. 1. The diagrams for the $\Lambda_c^+ \to \bar{K}^0 MB$ decay.

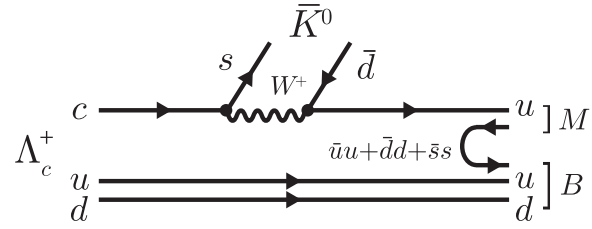

FIG. 2. The quark-level diagram for the $\Lambda_c^+ \to \bar{K}^0 MB$ process.

PB channels with an off-shell approach that is equivalent to considering different subtraction constants from those in Ref. [34].

Nonleptonic weak decays have been widely explored with the objective of studying and testing the properties of baryonic resonances [42–48], thus allowing for a way to distinguish between the different models used to generate them. For example, in Ref. [45] the decay $\Lambda_c^+ \to \pi^+\pi\Sigma$ was studied to get the $\pi\Sigma$ scattering lengths. In Ref. [44] the $\Lambda_c^+ \to \pi^+ MB$ decay, with the M a meson and B a baryon for $MB = \pi\Sigma, \bar{K}N$, and $\eta\Lambda$ was studied to better understand the $\Lambda(1405)$ and $\Lambda(1670)$ properties, and in Ref. [46] the $\Lambda_c^+ \to \eta\pi^+\Lambda$ was used to investigate the $a_0(980)$ and $\Lambda(1670)$ resonances. With this in mind, in Ref. [48] the $\Lambda_c^+ \to \bar{K}^0\eta p$ decay was used to study the nature of the $N^*(1535)$ by comparing different models, including the one in Ref. [30]. In that study, only PB channels were considered in this process, which corresponds to ignoring the influence that the VB channels can have in the nonleptonic decay through a large coupling of the $N^*(1535)$ to the ρN channel, as found in Ref. [34]. Indeed, the effect of the VB channel can be quite large in some reactions as was shown in Refs. [49,50].

In this paper we extend the calculations done in Ref. [48] to take into account the VB channels, and the effects of the $N^*(1650)$ resonance, using the model developed in Ref. [34]. Using this we calculate the mass distribution of ηN in the $\Lambda_c^+ \to \bar{K}^0\eta p$ decay and the mass distribution of πN and $K\Sigma$ in the $\Lambda_c^+ \to \bar{K}^0\pi N$ and $\Lambda_c^+ \to \bar{K}^0 K\Sigma$ decays. In this way we hope to shed some light on the nature of the $N^*(1535)$ as well as the $N^*(1650)$.

The paper is organized as follows. The theoretical framework of this study, the weak process of $\Lambda_c^+ \to \bar{K}^0 MB$ and the meson-baryon scattering amplitude, is given in Sec. II. Section III is devoted to the results, the mass distribution of the $\Lambda_c^+ \to \bar{K}^0 MB[MB = \pi N(I = 1/2), \eta p$ and $K\Sigma(I = 1/2)]$. A summary of this work is given in Sec. IV.

II. FORMALISM

The diagrams for the Λ_c^+ decay into $\bar{K}^0 MB$ that we take into account in this study are depicted in Fig. 1. The primary $\bar{K}^0 MB$ production in the Λ_c^+ decay occurs in the weak process and it is followed by the rescattering of the meson-baryon pair MB where, as studied in Ref. [34], the resonances $N^*(1535)$ and $N^*(1650)$ are generated through the dynamics of hadrons.

First, we discuss the primary vertex of the Λ_c^+ decay into $\bar{K}^0 MB$. In this process, we use the same approach as done in Ref. [48], but now we have an additional ρN channel. We consider the diagram shown in Fig. 2 for the weak transition and the hadronization at the quark level. The reaction can occur with the intermediate W^+ exchange with the Cabibbo-allowed coupling of W^+ to cs and $\bar{d}u$ [51], with a sequential pair creation of the light quark from the vacuum. The $\bar{d}s$ pair forms the $\bar{K}^0$, and the remaining uud quarks with a $\bar{q}q$ from the vacuum hadronize into the meson-baryon pair. In this approach, the ud pair in Λ_c^+ with the spin $S = 0$ and isospin $I = 0$ acts as a spectator. Then, at the quark level we can write the final state as

$$u(\bar{u}u + \bar{d}d + \bar{s}s)\frac{1}{\sqrt{2}}(ud - du) = \sum_i M_{1i} q_i \frac{1}{\sqrt{2}}(ud - du), \tag{1}$$

where $M_{ij} = q_i\bar{q}_j$ ($q_1 = u, q_2 = d, q_3 = s$). The matrix M at the quark level can be related with that at the hadronic level based on the flavor symmetry. Then, the matrix M for the pseudoscalar meson is given by [50]

$$M = \begin{pmatrix} \frac{\pi^0}{\sqrt{2}} + \frac{\eta}{\sqrt{3}} + \frac{\eta'}{\sqrt{6}} & \pi^+ & K^+ \\ \pi^- & -\frac{\pi^0}{\sqrt{2}} + \frac{\eta}{\sqrt{3}} + \frac{\eta'}{\sqrt{6}} & K^0 \\ K^- & \bar{K}^0 & -\frac{\eta}{\sqrt{3}} + \sqrt{\frac{2}{3}}\eta' \end{pmatrix}, \tag{2}$$

which contains the η, η' mixing of Ref. [52], and we obtain

$$\begin{aligned} &\sum_i M_{1i} q_i \frac{1}{\sqrt{2}}(ud - du) \\ &= \left(\frac{\pi^0}{\sqrt{2}} + \frac{\eta}{\sqrt{3}}\right) u\frac{1}{\sqrt{2}}(ud - du) + \pi^+ d\frac{1}{\sqrt{2}}(ud - du) \\ &\quad + K^+ s\frac{1}{\sqrt{2}}(ud - du). \end{aligned} \tag{3}$$

Referring to Ref. [53] for the quark representation of the baryons (see also footnote 1 in Ref. [50]),

$$p = \frac{u(ud - du)}{\sqrt{2}}, \tag{4}$$

$$n = \frac{d(ud - du)}{\sqrt{2}}, \tag{5}$$

$$\Lambda = \frac{u(ds - sd) + d(su - us) - 2s(ud - du)}{2\sqrt{3}}, \tag{6}$$

TABLE I. Coefficients h_{MB} and f_{MB} in Eq. (13).

	$\pi N(I=1/2)$	ηN	$K\Lambda$	$\rho N(I=1/2)$
h_{MB}	$-\sqrt{\frac{3}{2}}$	$\frac{1}{\sqrt{3}}$	$-\sqrt{\frac{2}{3}}$	$-\sqrt{\frac{3}{2}}$
f_{MB}	$\frac{1}{4\pi}\frac{1}{2}$	$\frac{1}{4\pi}\frac{1}{2}$	$\frac{1}{4\pi}\frac{1}{2}$	$\frac{1}{4\pi}\frac{1}{2\sqrt{3}}$

we can write the final state of the pseudoscalar meson and baryon $|PB\rangle$, apart from the $\bar{K}^0$ meson, as

$$\begin{aligned}|PB\rangle &= \frac{1}{\sqrt{2}}|\pi^0 p\rangle + \frac{1}{\sqrt{3}}|\eta p\rangle + |\pi^+ n\rangle - \sqrt{\frac{2}{3}}|K^+\Lambda\rangle \\ &= -\sqrt{\frac{3}{2}}|\pi N(I=1/2)\rangle + \frac{1}{\sqrt{3}}|\eta p\rangle - \sqrt{\frac{2}{3}}|K^+\Lambda\rangle,\end{aligned} \tag{7}$$

where the πN channel is written in terms of the isospin basis ($|\pi^+\rangle = -|I=1, I_z=1\rangle$ in this convention). Here, we have omitted the $\eta' p$ channel because the threshold is far above the energy of the $N^*(1535)$ and $N^*(1650)$ that we focus on in this study. In the same way, replacing the matrix M with the matrix V for the vector mesons [37],

$$V = \begin{pmatrix} \frac{\rho^0}{\sqrt{2}} + \frac{\omega}{\sqrt{2}} & \rho^+ & K^{*+} \\ \rho^- & -\frac{\rho^0}{\sqrt{2}} + \frac{\omega}{\sqrt{2}} & K^{*0} \\ K^{*-} & \bar{K}^{*0} & \phi \end{pmatrix}, \tag{8}$$

where the ideal mixing of the isospin-singlet mesons is assumed, we can obtain the final state with a vector meson $|VB\rangle$ as

$$|VB\rangle = -\sqrt{\frac{3}{2}}|\rho N(I=1/2)\rangle. \tag{9}$$

Here, the irrelevant channels containing the ω, ϕ, K^*, and $\bar{K}^*$ mesons are omitted and the phase convention $|\rho^+\rangle = -|I=1, I_z=1\rangle$ should be understood.

Combining these two cases in Eqs. (7) and (9), we can write the hadronic final state except for the $\bar{K}^0$ meson $|MB\rangle$ as

$$\begin{aligned}|MB\rangle &= -\sqrt{\frac{3}{2}}|\pi N(I=1/2)\rangle + \frac{1}{\sqrt{3}}|\eta p\rangle - \sqrt{\frac{2}{3}}|K^+\Lambda\rangle \\ &\quad - \sqrt{\frac{3}{2}}|\rho N(I=1/2)\rangle \\ &\equiv \sum_{MB} h_{MB}|MB\rangle,\end{aligned} \tag{10}$$

where the coefficient of each channel h_{MB} stands for the relative production weight from the Λ_c^+ and is summarized in Table I. The weight of the ρN channel in Eq. (10) is only due to flavor. In addition a different spin structure of the pseudoscalar and vector meson leads to a different factor for the production weight in the decay process, as was studied in Refs. [49,50] based on the $^3P_0$ model for the hadronization. Now, we only need to see the $J=1/2$ case because the resonances $N^*(1535)$ and $N^*(1650)$ have $J^P = 1/2^-$. Because the $q\bar{q}$ should have $J^P = 0^+$ which are the same quantum numbers as those of the vacuum, the total angular momentum after the hadronization should come from that of the u quark from the weak vertex that is denoted by $|J, M; u\rangle$. According to the $^3P_0$ model [54–56], the angular momentum L should be $L=1$ for parity conservation, and at the same time the spin S should be $S=1$ to have $J=0$ by addition with $L=1$. This is written as $|0,0;\bar{q}q\rangle_{^3P_0}$. The ud pair in the Λ_c^+, or equivalently in the final state baryon, has spin $J=0$ and isospin $I=0$ that is written as $|0,0;ud\rangle_{\text{spectator}}$. Following the works of Refs. [49,50], writing the relative angular momentum between the produced u quark from the weak vertex and $\bar{q}$ of the $\bar{q}q$ from the vacuum in the final state as j, we can rewrite the spin structure of the system as

$$\begin{aligned}&|J, M; u\rangle|0,0;\bar{q}q\rangle_{^3P_0}|0,0;ud\rangle_{\text{spectator}} \\ &\quad = \sum_j \mathcal{C}(j,J)|J, M, j\rangle.\end{aligned} \tag{11}$$

Now, the $j=0$ and 1 cases correspond to the pseudoscalar and vector meson production, respectively. Then, since we are only interested in the $J=1/2$ case, we can write

$$\begin{aligned}&\left|\frac{1}{2}, \pm\frac{1}{2}; u\right\rangle|0,0;\bar{q}q\rangle_{^3P_0}|0,0;ud\rangle_{\text{spectator}} \\ &\quad = \sum_{MB} f_{MB}\left|\frac{1}{2}, \pm\frac{1}{2}; MB\right\rangle,\end{aligned} \tag{12}$$

where the factor f_{MB} is $\frac{1}{4\pi}\frac{1}{2}$ and $\frac{1}{4\pi}\frac{1}{2\sqrt{3}}$ for the cases with M the pseudoscalar meson and the vector meson, respectively, and we show it in Table I.

Then, we can write the decay amplitude of the tree-level diagram given in Fig. 1(a) as

$$t_{\Lambda_c \to \bar{K}^0 MB} = V_P h_{MB} f_{MB}, \tag{13}$$

where V_P is a common constant for the strength of the production and the coefficients h_{MB} and f_{MB} are the factors originating from the flavor and spin structures given in Eqs. (10) and (12) (see Table I). In this study, we omit the possible energy dependence of the amplitude because the reaction proceeds in s wave and, as we will see later, only a small energy range around the $N^*(1535)$ and $N^*(1650)$ resonances is of our interest.

In this approach, the $\pi\Delta$ and $K\Sigma$ productions are suppressed because the ud pair in Λ_c^+, which has spin $S=0$ and isospin $I=0$, is a spectator, i.e., the spin and isospin structure of the ud pair is not changed throughout the hadronization process. While there are other possibilities for the creation of the quark pair which enable us to have the $K\Sigma$ or $\pi\Delta$ production, the study of Ref. [57] suggests that in the case of $\Lambda_b^0 \to J/\psi\pi^- p$, which has the same topology as the diagram of the weak process studied here, the spectator treatment gives a good description for the experimental data of Ref. [58]. Then, we expect that this treatment also works well in the present case.

For the meson-baryon amplitude $t_{MB,M'B'}$ in Fig. 1(b), which is responsible for the rescattering after the hadronization, we follow the study of Ref. [34]. In the study, the meson-baryon amplitude was evaluated by using the chiral unitary approach with the πN, ηN, $K\Lambda$, $K\Sigma$, ρN, and $\pi\Delta(d$ wave)

channels, and it was found that the $N^*(1535)$ and $N^*(1650)$ resonances are dynamically generated. The interaction kernel of PB to PB and VB to VB is given by the leading order of the chiral Lagrangian, or equivalently the vector meson exchange [30,37], and the transition of PB to VB is taken into account through the one pion exchange and the Kroll-Ruderman term [38,39].[1] Then, writing the interaction kernel as v, the meson-baryon amplitude $t_{MB,M'B'}$ is given by

$$t_{MB,M'B'} = [(1 - vG)^{-1}v]_{MB,M'B'}, \tag{14}$$

where G is the meson-baryon loop function evaluated with dimensional regularization. The analytic form of the loop function of the MB channel, $G_{MB}(\sqrt{s},m_M,M_B)$, is given by

$$\begin{aligned} &G_{MB}(\sqrt{s},m_M,M_B) \\ &= \frac{2M_B}{16\pi^2}\left\{a_{MB}(\mu) + \ln\frac{M_B^2}{\mu^2} + \frac{m_M^2 - M_B^2 + s}{2s}\ln\frac{m_M^2}{M_B^2}\right. \\ &+ \frac{q_{MB}}{\sqrt{s}}\left[\ln\left(s - M_B^2 + m_M^2 + 2q_{MB}\sqrt{s}\right)\right. \\ &+ \ln\left(s + M_B^2 - m_M^2 + 2q_{MB}\sqrt{s}\right) \\ &- \ln\left(-s + M_B^2 - m_M^2 + 2q_{MB}\sqrt{s}\right) \\ &\left.\left. - \ln\left(-s - M_B^2 + m_M^2 + 2q_{MB}\sqrt{s}\right)\right]\right\}, \end{aligned} \tag{15}$$

with μ the regularization scale, m_M and M_B the mass of the meson and baryon, respectively, and q_{MB} the meson momentum in the meson-baryon center-of-mass (CM) frame $q_{MB} = \lambda^{1/2}(s,m_M^2,M_B^2)/2\sqrt{s}$ where $\lambda(x,y,z) = x^2 + y^2 + z^2 - 2xy - 2yz - 2zx$.

Finally, the decay amplitude of the $\Lambda_c^+ \to \bar{K}^0 MB$ process from the diagrams in Figs. 1(a) and 1(b) is given by

$$\begin{aligned} &t_{\Lambda_c^+\to\bar{K}^0 MB} \\ &= V_P h_{MB} f_{MB} + \sum_{M'B'} V_P h_{M'B'} f_{M'B'} G_{M'B'} \\ &\quad \times (M_{M'B'}) t_{M'B',MB}(M_{MB}), \end{aligned} \tag{16}$$

where M_{MB} denotes the invariant mass of the meson M and baryon B (now $M_{MB} = M_{M'B'}$). Regarding the meson-baryon loop function G_{MB} following the tree-level amplitude for $\Lambda_c^+ \to \bar{K}^0 M'B'$ and before $t_{M'B',MB}$ in Fig. 1(b), we use the same subtraction constants as those in the meson-baryon amplitude $t_{MB,M'B'}$ given in Ref. [34]. In the same way as done in Refs. [34,38] we use the ρN loop function $\tilde{G}_{\rho N}$ which is obtained by smearing the loop function $G_{\rho N}(\sqrt{s},m_\rho,M_N)$ given by Eq. (15) with the ρ-meson spectral function to take account of the width of the ρ meson,[2]

$$\begin{aligned} &\tilde{G}_{\rho N}(\sqrt{s}) \\ &= \frac{1}{N}\int_{m_\rho - 2\Gamma_\rho}^{m_\rho + 2\Gamma_\rho} 2\tilde{m}d\tilde{m}\left(-\frac{1}{\pi}\right)\mathrm{Im}\left[\frac{1}{\tilde{m}^2 - m_\rho^2 + i\tilde{m}\Gamma_\rho(\tilde{m})}\right] \\ &\quad \times G_{\rho N}(\sqrt{s},\tilde{m},M_N), \end{aligned} \tag{17}$$

with

$$\Gamma_\rho(\tilde{m}) = \Gamma_\rho \frac{|\vec{q}\,|^3}{|\vec{q}\,|_{\rm on}^3}\theta(\tilde{m} - 2m_\pi), \tag{18}$$

$$|\vec{q}\,| = \frac{\lambda^{1/2}\left(\tilde{m}^2,m_\pi^2,m_\pi^2\right)}{2\tilde{m}}, \tag{19}$$

$$|\vec{q}\,|_{\rm on} = \frac{\lambda^{1/2}\left(m_\rho^2,m_\pi^2,m_\pi^2\right)}{2m_\rho}, \tag{20}$$

$$\begin{aligned} N = &\int_{m_\rho - 2\Gamma_\rho}^{m_\rho + 2\Gamma_\rho} 2\tilde{m}d\tilde{m}\left(-\frac{1}{\pi}\right) \\ &\times \mathrm{Im}\left[\frac{1}{\tilde{m}^2 - m_\rho^2 + i\tilde{m}\Gamma_\rho(\tilde{m})}\right]. \end{aligned} \tag{21}$$

Here, we note that the $K\Sigma$ and $\pi\Delta$ channels are not included in the sum of $M'B'$ in Eq. (16) because there is no direct production from Λ_c^+ in our approach in Eq. (10), while these channels appear in the meson-baryon amplitude $t_{MB,M'B'}$.

With an appropriate phase-space factor, the mass distribution $d\Gamma_{\Lambda_c^+\to\bar{K}^0 MB}/dM_{MB}$ as a function of M_{MB} is given by

$$\frac{d\Gamma_{\Lambda_c^+\to\bar{K}^0 MB}}{dM_{MB}} = \frac{1}{(2\pi)^3}\frac{M_B}{M_{\Lambda_c^+}}|\vec{p}_{\bar{K}^0}||\vec{\tilde{p}}_M||t_{\Lambda_c^+\to\bar{K}^0 MB}|^2, \tag{22}$$

where $p_{\bar{K}^0}$ and $\tilde{p}_M$ are the momentum of $\bar{K}^0$ in the Λ_c^+ rest frame and that of the meson M in the MB CM frame, respectively, with

$$|\vec{p}_{\bar{K}^0}| = \frac{\lambda^{1/2}\left(M_{\Lambda_c^+}^2,m_{\bar{K}^0}^2,M_{MB}^2\right)}{2M_{\Lambda_c^+}}, \tag{23}$$

$$|\vec{\tilde{p}}_M| = \frac{\lambda^{1/2}\left(M_{MB}^2,m_M^2,M_B^2\right)}{2M_{MB}}. \tag{24}$$

Here, we give a comment on the possible modification of the mass distribution by the rescattering of $\bar{K}^0$ with the meson M or baryon B in the final state, which are not taken into account in this study. The $\bar{K}^0 p$ in the $\Lambda_c^+ \to \bar{K}^0\eta p$ decay can couple to some Σ^* resonances, but as pointed out in Ref. [48], these resonances would not give a large modification to the mass distribution because of the small overlap with the phase space and the p-wave coupling of the Σ^* to the $\bar{K}^0 p$ channel. Another possibility is the coupling of $K\bar{K}$ with the $a_0(980)$ or $f_0(980)$ states in the $\Lambda_c^+ \to \bar{K}^0 K\Lambda$ or $\bar{K}^0 K\Sigma$ decays. In this case, the invariant mass of the $\bar{K}^0 K$ pair spreads up in a range of invariant masses above 1050 MeV, and then the overlap of

[1] In practice, to obtain the same result to Ref. [34], we add the contact and Born terms to the diagonal ρN channel of the interaction kernel as in Ref. [41], and the energy transfer in the one pion exchange diagram is omitted in this calculation.

[2] We note that the real part of the ρN loop function becomes positive below the ρN threshold with the subtraction constant in Ref. [34].

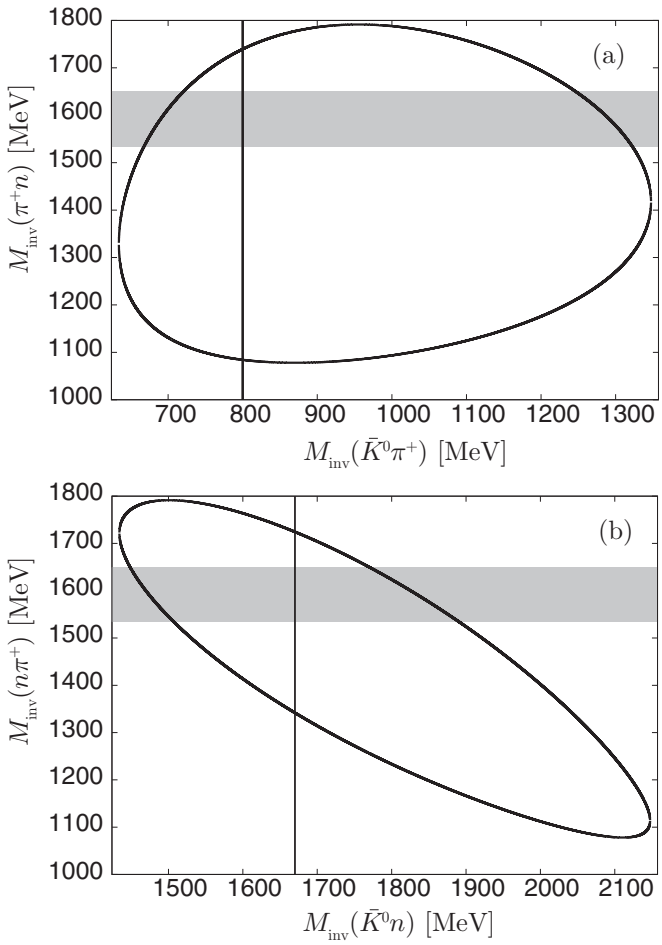

FIG. 3. Dalitz plots for $\bar{K}^0\pi^+ n$ showing $M_{\rm inv}(\pi^+ n)$ versus $M_{\rm inv}(\bar{K}^0\pi^+)$ for the case (a) and $M_{\rm inv}(n\pi^+)$ versus $M_{\rm inv}(\bar{K}^0 n)$ for the case (b). The shaded areas are the energies of $N^*(1535)$ and $N^*(1650)$ which we are interested in. The vertical lines in (a) and (b) correspond to the masses of $\kappa(800)$ and $\Lambda(1670)$, respectively.

the $a_0(980)$ and $f_0(980)$ resonances with the $\Lambda_c^+ \to \bar{K}^0 K\Lambda$ or $\bar{K}^0 K\Sigma$ phase space is small. Though some Λ^* resonances can also contribute in the $\Lambda_c^+ \to \bar{K}^0\pi N$ process through the $\bar{K}^0 N$ rescattering, it does not matter in our case because now we are interested in the mass distribution as a function of $M_{\pi N}$, not $M_{\bar{K}^0 N}$, where the Λ^* distributes its strength. Then, a resonance such as $\Lambda(1800)$ [4], which can have a certain overlap with the phase space in $d^2\Gamma_{\Lambda_c^+\to\bar{K}^0\pi N}/dM_{\pi N}dM_{\bar{K}^0 N}$, is integrated over in $M_{\bar{K}N}$ and gives just a broad background in the $M_{\pi N}$ mass distribution.

To clarify further this issue, we show in Fig. 3 two examples of what happens to the interaction of $\bar{K}^0\pi$ or $\bar{K}^0 N$ in the $\Lambda_c^+ \to \bar{K}^0\pi N$ reaction (we take the $\Lambda_c^+ \to \bar{K}^0\pi^+ n$ reaction, as an example). In Fig. 3, we show two Dalitz plots for this reaction, one showing $M_{\rm inv}(\pi^+ n)$ versus $M_{\rm inv}(\bar{K}^0\pi^+)$ and another one showing $M_{\rm inv}(n\pi^+)$ versus $M_{\rm inv}(\bar{K}^0 n)$. In the first case, the $\bar{K}^0\pi^+$ can lead to the $\kappa(800)$ resonance in s wave. This resonance is very broad, and furthermore, as can be seen in Fig. 3(a), the strength of this resonance is spread out in a range of values of $M_{\rm inv}(\pi^+ n)$ from 1100 MeV to about 1750 MeV. Then the effect of this resonance in the $\bar{K}^0\pi^+$ channel is spread out over 650 MeV of $M_{\rm inv}(\pi^+ n)$ and its effects are totally diluted, contributing with a small and smooth background to the $M_{\rm inv}(\pi^+ n)$ distribution. The case in Fig. 3(b) is similar. Here, we plot $M_{\rm inv}(n\pi^+)$ versus $M_{\rm inv}(\bar{K}^0 n)$. Now in s wave we can have three resonances of $\bar{K}^0 n$, either of the two $\Lambda(1405)$ and the $\Lambda(1670)$. The two $\Lambda(1405)$ resonances are below the $\bar{K}N$ threshold, but the $\Lambda(1670)$ could in principle contribute. Once again we see that for this value of the $\bar{K}^0 n$ invariant mass the values of $M_{\rm inv}(n\pi^+)$ range from about 1350 to 1730 MeV, nearly 400 MeV span where the effect of the $\Lambda(1670)$ (relatively weak) would be also spread out, leading to a smooth background below the πN resonance peaks of $N^*(1535)$ and $N^*(1650)$.

TABLE II. The absolute values of $g_{N^*,M'B'}G_{M'B'}$ (in MeV) at the resonance pole, taken from Ref. [34].

	πN	ηN	$K\Lambda$	$K\Sigma$	ρN	$\pi\Delta$
$N^*(1535)$	25.2	42.2	40.7	3.2	17.9	8.8
$N^*(1650)$	36.6	34.0	20.3	31.6	8.1	9.0

III. RESULTS

The mass distributions $d\Gamma_{\Lambda_c^+\to\bar{K}^0 MB}/dM_{MB}$ with $MB = \pi N(I=1/2), \eta p$, and $K\Sigma(I=1/2)$ as functions of M_{MB} are given in Fig. 4. In these figures, we show the results with $V_P = 1\,\text{MeV}^{-1}$ because of our lack of the knowledge to fix the value of V_P. This is not a problem since we only want to focus on the behavior of the mass distribution.

For the πN mass distribution of the $\Lambda_c^+ \to \bar{K}^0\pi N$ decay, we can see two peaks; the peak located in the lower energy, which is associated with the $N^*(1535)$ resonance, has larger strength than the one in the higher energy which comes from the $N^*(1650)$. However, in the scattering amplitude of the diagonal πN channel in Ref. [34], the magnitude of the higher peak is larger than that of the lower peak. We can understand this difference from the coupling of the resonances with the meson-baryon states given in Ref. [34]. Indeed, $g_{N^*(1535),\pi N} = 1.03 + i0.21$ versus $g_{N^*(1650),\pi N} = 1.37 + i0.54$. Then, the Breit-Wigner amplitude $g^2_{R,\pi N}/(\sqrt{s} - M_R + i\Gamma_R/2)$ has larger strength in the case of the $N^*(1650)$. However, if we write the meson-baryon amplitude with the Breit-Wigner amplitude (see Fig. 5 for the diagram), the $\Lambda_c^+ \to \bar{K}^0 MB$ amplitude T_{BW} is given by

$$T_{BW} = \sum_{N^*}\sum_{M'B'} V_P h_{M'B'} f_{M'B'} G_{M'B'}(M_{M'B'}) \times \frac{g_{N^*,M'B'}g_{N^*,MB}}{M_{MB} - M_{N^*} + i\Gamma_{N^*}/2}, \quad (25)$$

where the sum of N^* runs over $N^*(1535)$ and $N^*(1650)$. Then, the difference of the intermediate states appears in the combination of $g_{N^*,M'B'}G_{M'B'}$ around the resonance peak. We compare the absolute values of $g_{N^*,M'B'}G_{M'B'}$, given here in Table II, to get a rough understanding. The value of $g_{N^*,MB}G_{MB}$ for the ηN and $K\Lambda$ channels is larger for $N^*(1535)$ than $N^*(1650)$, while the magnitude of the coupling

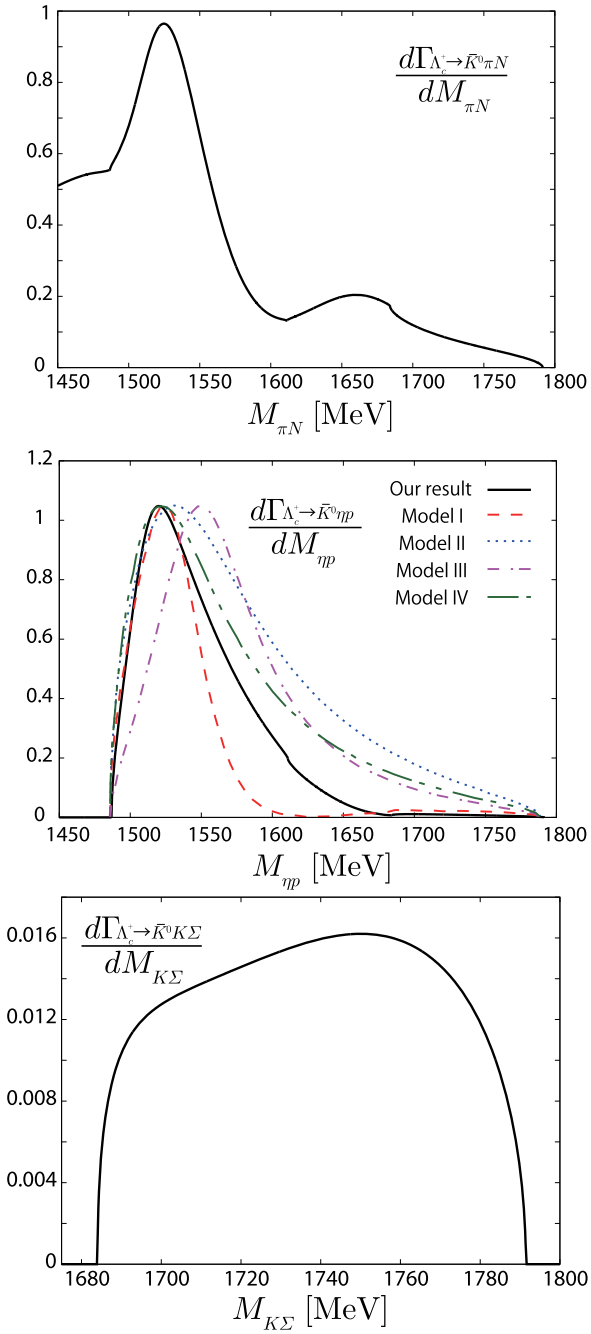

FIG. 4. The mass distributions for Λ_c^+ decay into $\bar{K}^0\pi N$ with $I = 1/2$ (top), $\bar{K}^0\eta p$ (middle), and $\bar{K}^0 K\Sigma$ with $I = 1/2$ (bottom) as functions of M_{MB}. In the middle figure, the lines other than the solid one are the results given in Ref. [48] with the height scaled to agree with the result of this study.

of the πN channel to $N^*(1650)$ is larger than the coupling to $N^*(1535)$. Furthermore, in the primary vertex the $K\Sigma$ channel which has a larger coupling to $N^*(1650)$ than $N^*(1535)$ is not produced. As the result, the peak of the $N^*(1535)$ resonance is larger than that of the $N^*(1650)$ in the mass distribution of Λ_c^+ decay into $\bar{K}^0\pi N$.

At the middle of Fig. 4, we show the ηp invariant mass distribution in the $\Lambda_c^+ \to \bar{K}^0\eta p$ process with the result of

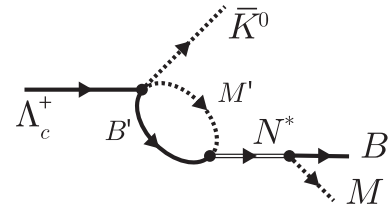

FIG. 5. The diagram from the resonance for the $\Lambda_c^+ \to \bar{K}^0 MB$.

Ref. [48] for comparison. In this case, we can see only a single peak. Compared with the mass distribution of Model I in Ref. [48], the mass distribution has a larger width. This would be attributed to the effect of the $N^*(1650)$, analogously to the amplitude of the πN to ηN reaction in Ref. [34], where a single peak is observed in the cross section and its larger width than in Ref. [30] is ascribed to the $N^*(1650)$. However, the contribution from the $N^*(1650)$ is more suppressed than that in the $\Lambda_c^* \to \bar{K}^0\pi N$ process because of the stronger coupling of the ηN channel to the $N^*(1535)$ than $N^*(1650)$ In addition, the absence of the $K\Sigma$ channel in the initial production process [see Eq. (10)], also weakens the strength of the $N^*(1650)$ because, while gG for this channel is stronger for $N^*(1650)$ than for $N^*(1535)$ (see Table II), the present process cannot be initiated by the $K\Sigma$ channel. However, the mass distribution in Fig. 4 still has a larger width compared to the mass distribution of the Model I in Ref. [48], where only the $N^*(1535)$ is included following the work of Ref. [30] using the chiral unitary approach without the $\rho N(I = 1/2)$ and $\pi\Delta(d$ wave) channels. Meanwhile, the width of the mass distribution of the $\Lambda_c^+ \to \bar{K}^0\eta p$ is smaller than those of Models II, III, and IV in Ref. [48]. In these models, the $N^*(1535)$ is treated as a Breit-Wigner amplitude and its width is larger than that obtained in Refs. [30,34] or has energy dependence which makes the width effectively large at higher energy.

For completeness, the $K\Sigma$ mass distribution of the $\Lambda_c^+ \to \bar{K}^0 K\Sigma$ decay is shown at the bottom of Fig. 4. In Ref. [34], the value of $g_{N^*,K\Sigma}G_{K\Sigma}$ is larger for the $N^*(1650)$ resonance than the $N^*(1535)$ resonance, and the $N^*(1535)$ energy is about 200 MeV below the $K\Sigma$ threshold. Then, we can expect that the $K\Sigma$ production is mainly driven by the $N^*(1650)$ resonance. However, as given in Eq. (10) the $K\Sigma$ pair is not produced directly from the Λ_c decay. Then, the $K\Sigma$ pair is produced only through the coupled channel effect of the meson-baryon amplitude $t_{MB,M'B'}$ in our approach, and the magnitude of the mass distribution is much smaller compared with that of πN or ηN.

In Fig. 6, we show the mass distribution omitting the ρN channel in the sum of $M'B'$ in Eq. (16). The ρN channel contributes in a destructive way to the mass distribution. In the πN case, the effect of the ρN channel looks more significant for the lower peak. This is because, as shown in Ref. [34], the ρN channel has a larger value of $g_{N^*,\rho N}G_{\rho N}$ for the $N^*(1535)$ resonance than for the $N^*(1650)$ resonance.

Thus, in the Λ_c^+ decay into $\bar{K}^0 MB$ [$MB = \pi N(I = 1/2), \eta p$ and $K\Sigma(I = 1/2)$] the resonances $N^*(1535)$ and $N^*(1650)$ appear in a different way than in the meson-

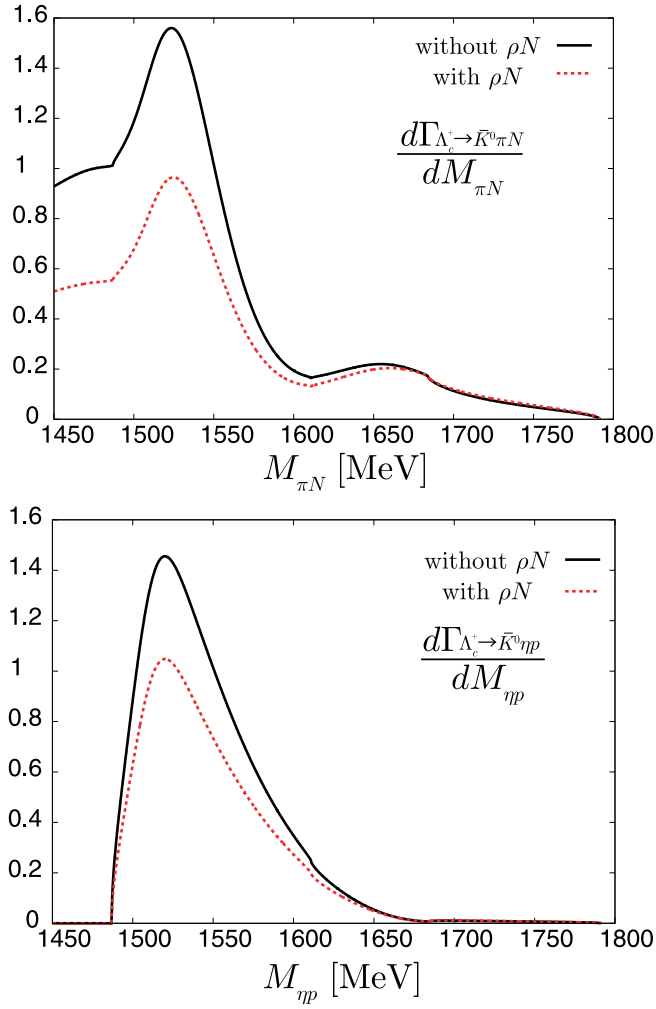

FIG. 6. The mass distribution for $\Lambda_c^+ \to \bar{K}^0\pi N$ with $I = 1/2$ (top) and $\bar{K}^0\eta p$ (bottom) without ρN channel. The mass distributions with the ρN channel are shown with the dotted lines.

baryon amplitude in Ref. [34]. In addition, we found a difference from the models which do not contain the $N^*(1650)$ or with respect the five-quark models of the $N^*(1535)$ that were discussed in Ref. [48]. Then, the production of the $N^*(1535)$ and $N^*(1650)$ from the Λ_c^+ decay is a good process to clarify the properties of the $N^*(1535)$ and $N^*(1650)$ resonances.

IV. SUMMARY

We have studied the mass distribution of the $\Lambda_c^+ \to \bar{K}^0 MB$ [$MB = \pi N(I = 1/2)$, ηp, and $K\Sigma(I = 1/2)$] including the effect of the $N^*(1535)$ and $N^*(1650)$ resonances which are generated by the hadron dynamics with the πN, ηN, $K\Lambda$, $K\Sigma$, ρN, and $\pi\Delta(d$ wave) channels as investigated in Ref. [34]. While both effects of the $N^*(1535)$ and $N^*(1650)$ are seen in the mass distributions, we found that their manifestation is different from that in the meson-baron amplitude given in Ref. [34], or experiment. In our mass distribution for $\Lambda_c^+ \to \bar{K}^0\pi p(I = 1/2)$ and $\bar{K}^0\eta p$, the peak from $N^*(1535)$ is larger than that from $N^*(1650)$, while two peaks with a comparable magnitude are seen in the amplitude of the πN to πN channel in Ref. [34]. This is because the $K\Sigma$ channel which couples more strongly to $N^*(1650)$ than $N^*(1535)$ is suppressed in the primary production from Λ_c^+ in our treatment of the weak and hadronization processes and the $\rho N(I = 1/2)$ and $K\Lambda$ channels have larger couplings to the $N^*(1535)$ resonance than the $N^*(1650)$ resonance.

Furthermore, we find differences from the treatment of the $N^*(1535)$ made in Ref. [48], where a five-quark component of the $N^*(1535)$ is included using a Breit-Wigner amplitude.

In the case of $MB = K\Sigma(I = 1/2)$, the $N^*(1650)$ resonance is expected to give a dominant contribution to the production amplitude, but we found that the magnitude of the mass distribution of the $\Lambda_c^+ \to \bar{K}^0 K\Sigma(I = 1/2)$ is much smaller than for the other processes, like $\Lambda_c^+ \to \bar{K}^0\eta p$, because the production of the $K\Sigma$ is suppressed in the weak and hadronization process.

The subtleties and results in the different channels in the reactions studied here are tied to the nature of the $N^*(1535)$ and $N^*(1650)$ resonances as dynamically generated from the hadron interaction in coupled channels, and the experimental observation of these decay modes should bring new information concerning the nature of these states.

ACKNOWLEDGMENTS

R.P. thanks the Generalitat Valenciana in the program Santiago Grisolia. This work is partly supported by the Spanish Ministerio de Economia y Competitividad and European FEDER funds (Fondo Europeo de Desarrollo Regional) under Contracts No. FIS2014-57026-REDT, No. FIS2014-51948-C2-1-P, and No. FIS2014-51948-C2-2-P, and the Generalitat Valenciana in the program Prometeo II-2014/068.

[1] E. Klempt and A. Zaitsev, Phys. Rep. **454**, 1 (2007).
[2] V. Crede and W. Roberts, Rep. Prog. Phys. **76**, 076301 (2013).
[3] S. Capstick and W. Roberts, Prog. Part. Nucl. Phys. **45**, S241 (2000).
[4] C. Patrignani *et al.*, [Particle Data Group], Chin. Phys. C **40**, 100001 (2016).
[5] B. C. Liu and B. S. Zou, Phys. Rev. Lett. **96**, 042002 (2006).
[6] L. Y. Glozman, W. Plessas, K. Varga, and R. F. Wagenbrunn, Phys. Rev. D **58**, 094030 (1998).
[7] R. Bijker, F. Iachello, and A. Leviatan, Ann. Phys. **236**, 69 (1994).
[8] C. Helminen and D. O. Riska, Nucl. Phys. A **699**, 624 (2002).
[9] C. S. An and B. S. Zou, Eur. Phys. J. A **39**, 195 (2009).
[10] J. Ferretti, R. Bijker, G. Galatá, H. García-Tecocoatzi, and E. Santopinto, Phys. Rev. D **94**, 074040 (2016).
[11] Z. P. Li, J. Phys. G **23**, 1127 (1997).
[12] M. Doring, E. Oset, and D. Strottman, Phys. Rev. C **73**, 045209 (2006).

[13] J. J. Xie, B. S. Zou, and H. C. Chiang, Phys. Rev. C **77**, 015206 (2008).
[14] X. Cao and X. G. Lee, Phys. Rev. C **78**, 035207 (2008).
[15] L. S. Geng, E. Oset, B. S. Zou, and M. Doring, Phys. Rev. C **79**, 025203 (2009).
[16] M. Doring, E. Oset, and B. S. Zou, Phys. Rev. C **78**, 025207 (2008).
[17] X. Cao, J. J. Xie, B. S. Zou, and H. S. Xu, Phys. Rev. C **80**, 025203 (2009).
[18] V. R. Debastiani, S. Sakai, and E. Oset, Phys. Rev. C **96**, 025201 (2017).
[19] N. Kaiser, T. Waas, and W. Weise, Nucl. Phys. A **612**, 297 (1997).
[20] N. Kaiser, P. B. Siegel, and W. Weise, Nucl. Phys. A **594**, 325 (1995).
[21] E. Oset and A. Ramos, Nucl. Phys. A **635**, 99 (1998).
[22] D. Jido, J. A. Oller, E. Oset, A. Ramos, and U. G. Meissner, Nucl. Phys. A **725**, 181 (2003).
[23] J. A. Oller and U. G. Meissner, Phys. Lett. B **500**, 263 (2001).
[24] C. García-Recio, J. Nieves, E. R. Arriola, and M. J. V. Vacas, Phys. Rev. D **67**, 076009 (2003).
[25] T. Hyodo and W. Weise, Phys. Rev. C **77**, 035204 (2008).
[26] T. Hyodo, D. Jido, and L. Roca, Phys. Rev. D **77**, 056010 (2008).
[27] T. Hyodo and D. Jido, Prog. Part. Nucl. Phys. **67**, 55 (2012).
[28] Y. Kamiya, K. Miyahara, S. Ohnishi, Y. Ikeda, T. Hyodo, E. Oset, and W. Weise, Nucl. Phys. A **954**, 41 (2016).
[29] J. Nieves and E. R. Arriola, Phys. Rev. D **64**, 116008 (2001).
[30] T. Inoue, E. Oset, and M. J. V. Vacas, Phys. Rev. C **65**, 035204 (2002).
[31] P. C. Bruns, M. Mai, and U. G. Meissner, Phys. Lett. B **697**, 254 (2011).
[32] D. Gamermann, C. Garcia-Recio, J. Nieves, and L. L. Salcedo, Phys. Rev. D **84**, 056017 (2011).
[33] K. P. Khemchandani, A. M. Torres, H. Nagahiro, and A. Hosaka, Phys. Rev. D **88**, 114016 (2013).
[34] E. J. Garzon, and E. Oset, Phys. Rev. C **91**, 025201 (2015).
[35] N. Kaiser, P. B. Siegel, and W. Weise, Phys. Lett. B **362**, 23 (1995).
[36] T. Hyodo, D. Jido, and A. Hosaka, Phys. Rev. C **78**, 025203 (2008).
[37] E. Oset and A. Ramos, Eur. Phys. J. A **44**, 445 (2010).
[38] E. J. Garzon, J. J. Xie, and E. Oset, Phys. Rev. C **87**, 055204 (2013).
[39] E. J. Garzon and E. Oset, Eur. Phys. J. A **48**, 5 (2012).
[40] K. P. Khemchandani, A. Martinez Torres, H. Kaneko, H. Nagahiro, and A. Hosaka, Phys. Rev. D **84**, 094018 (2011).
[41] K. P. Khemchandani, A. Martinez Torres, H. Nagahiro and A. Hosaka, Phys. Rev. D **85**, 114020 (2012).
[42] V. Crede and C. A. Meyer, Prog. Part. Nucl. Phys. **63**, 74 (2009).
[43] H. X. Chen, W. Chen, X. Liu, and S. L. Zhu, Phys. Rept. **639**, 1 (2016).
[44] K. Miyahara, T. Hyodo, and E. Oset, Phys. Rev. C **92**, 055204 (2015).
[45] T. Hyodo and M. Oka, Phys. Rev. C **84**, 035201 (2011).
[46] J.-J. Xie and L.-S. Geng, Eur. Phys. J. C **76**, 496 (2016).
[47] E. Oset *et al.*, Int. J. Mod. Phys. E **25**, 1630001 (2016).
[48] J. J. Xie and L. S. Geng, Phys. Rev. D **96**, 054009 (2017).
[49] W. H. Liang, M. Bayar, and E. Oset, Eur. Phys. J. C **77**, 39 (2017).
[50] R. P. Pavao, W.-H. Liang, J. Nieves, and E. Oset, Eur. Phys. J. C **77**, 265 (2017).
[51] L. L. Chau, Phys. Rept. **95**, 1 (1983).
[52] A. Bramon, A. Grau, and G. Pancheri, Phys. Lett. B **283**, 416 (1992).
[53] K. Miyahara, T. Hyodo, M. Oka, J. Nieves, and E. Oset, Phys. Rev. C **95**, 035212 (2017).
[54] L. Micu, Nucl. Phys. B **10**, 521 (1969).
[55] A. Le Yaouanc, L. Oliver, O. Pene, and J. C. Raynal, Phys. Rev. D **8**, 2223 (1973).
[56] F. E. Close, *An Introduction to Quarks and Partons* (Academic Press, New York, 1979).
[57] E. Wang, H. X. Chen, L. S. Geng, D. M. Li, and E. Oset, Phys. Rev. D **93**, 094001 (2016).
[58] R. Aaij *et al.* (LHCb Collaboration), J. High Energy Phys. 07 (2014) 103.